J Therm Anal Calorim (2010) 99:57–63
DOI 10.1007/s10973-009-0454-0

# Evaluation of thermodynamic and kinetic stability of $CuAlO_2$ and $CuGaO_2$

**Yuh Kumekawa · Motohiro Hirai · Yuhki Kobayashi · Satoshi Endoh · Eri Oikawa · Takuya Hashimoto**

Japan Symposium 2008


**Abstract** Thermodynamic and kinetic stabilities of $CuAlO_2$ and $CuGaO_2$ have been evaluated by using thermogravimetry and thermodynamic calculations. It has been revealed that $CuAlO_2$ and $CuGaO_2$ are not thermodynamically stable in air below 800 °C and 1,200 °C, respectively, and that the oxidation reaction, $4CuMO_2 + O_2 \rightarrow 2CuO + 2CuM_2O_4$ (M = Al, Ga), should occur if the reaction kinetics are high enough. However, rate constants and activation energies indicated slow kinetics of the oxidation reaction, showing kinetic stability of $CuMO_2$ even under some thermodynamically unstable temperatures and atmospheres. It was also concluded that $CuAlO_2$ showed higher thermodynamic and kinetic stability than $CuGaO_2$.

**Keywords** $CuAlO_2$ · $CuGaO_2$ · Ellingham diagram · Kinetic stability · TG-DTA · Thermodynamic stability

## Introduction

$CuMO_2$ (M = Al, Ga, In, transition metal ion and rare earth ion) with delafossite structure has attracted much interest for p-type transparent conducting oxide, p-type thermoelectric semiconductor, three-way catalyst of exhaust gas purification, and luminescent material and magnetic property [1–7]. Information on stability of $CuMO_2$ at high temperatures under various gas atmospheres is necessary not only for practical application at high temperatures, such as three-way catalyst or thermoelectric energy conversion device, but also for film preparation, which is inevitable for development of new optical and electrical devices. Although, it can be regarded that $CuMO_2$ has a problem on long-term stability since they include $Cu^+$ which should be thermodynamically unstable in air at room temperature [8], there have been few satisfying reports on their thermodynamic stability and no report on their variation with M in $CuMO_2$. Jacob and Alcock reported temperatures and oxygen partial pressures, $P(O_2)$, where three phases, $CuAl_2O_4$, $CuAlO_2$, and CuO, coexist from electromotive force (emf) measurements [9]. However, the $P(O_2)$ for their measurements were limited to higher than 0.21 atm. Bruce and Cann proposed phase relationship among $CuGaO_2$–$CuGa_2O_4$–CuO–$Cu_2O$ system [10] based on the emf measurements performed by Jacob and Alcock [11]. However, their preparation experiments did not show agreement with their proposed phase diagram. On the kinetic stability of $CuMO_2$ under temperatures and gas atmospheres where they are thermodynamically unstable, no article has appeared.

In this study, thermodynamic stability of $CuAlO_2$ and $CuGaO_2$ has been quantitatively evaluated with thermodynamic calculation by using program MALT-2 [12]. Also, their kinetic stability under thermodynamically unstable circumstances has been investigated by TG-DTA and X-ray diffraction measurements. The variation of both stabilities with M in $CuMO_2$ is described.

## Experimental

$CuAlO_2$ ceramic specimen was prepared by solid state reaction method. Nominal amount of CuO (99.9%, Furuuchi Chemistry Corp.) and $\alpha$-$Al_2O_3$ (99.99%, Furuuchi Chemistry Corp.) powders were mixed by using YSZ

Y. Kumekawa · M. Hirai · Y. Kobayashi · S. Endoh · E. Oikawa · T. Hashimoto (✉)
Department of Integrated Sciences in Physics and Biology, College of Humanities and Sciences, Nihon University, 3-25-40 Sakurajousui, Setagaya-ku, Tokyo 156-8550, Japan
e-mail: takuya@chs.nihon-u.ac.jp

(yttria stabilized zirconia) planet-type ball mill with 300 rpm for 3 h. After pressing the mixed powder into pellet with 20 mm diameter, the specimen was heated at 1,200 °C for 24 h in air. The color of the obtained specimen was light bluish white. The $CuGaO_2$ specimen was also synthesized by solid state reaction method of the mixture of $Cu_2O$ (99.9%, Furuuchi Chemistry Corp.) and $Ga_2O_3$ (99.9%, Furuuchi Chemistry Corp.) powders. After mixing nominal amount of $Cu_2O$ and $Ga_2O_3$ powders using YSZ planet-type ball mill with 300 rpm for 3 h, the pellet with 20 mm diameter was prepared by molding. The pellet was heated at 1,100 °C for 24 h in $N_2$ flow with $P(O_2)$ of about $10^{-4}$ atm. The color of the specimen was light greenish white. In both preparation processes, the heating and cooling rates were 200 °C/h.

The specimens were crushed into powder and subjected to X-ray diffraction measurements using Cu K$\alpha$ radiation (50 kV, 250 mA: Rigaku RINT-2500). It was revealed that the single phases of delafossite structure were obtained for the both specimens.

For estimation of thermodynamics stability, $CuAlO_2$ and $CuGaO_2$ pellets were annealed at 900 °C and 700 °C, respectively, for 12 h in air. The phases after the heat-treatment were identified by powder X-ray diffraction measurements at room temperature. From the identification, the chemical formula of decompose reaction was proposed. The thermodynamic calculations of the proposed reactions were carried out using program MALT-2 [12] in order to evaluate the thermodynamic stabilities of $CuAlO_2$ and $CuGaO_2$ under various gas atmospheres.

For analysis of kinetics of the proposed decompose reaction, apparatus for TG-DTA (TG 8120, Rigaku Co., Ltd.) was employed. By using alumina mortar, single phase of $CuAlO_2$ and $CuGaO_2$ pellets were crushed into powders, whose particle size and distribution were evaluated with laser diffraction particle size analyzer (SALD3000S, SHIMADZU Co., Ltd.). The powder of about 30 mg was loaded on TG-DTA using Pt pan and the temperature was set at the measurement level after heating at a rate of 100 °C/min. The variation of the mass at constant temperature by time in air was recorded.

TG-DTA curves of the $CuAlO_2$ and $CuGaO_2$ powders in air were measured for comparison. $Al_2O_3$ powder and Pt were employed for the reference and material of pan, respectively. Heating rate was 10 °C/min.

## Results and discussion

### Thermodynamic stability of $CuMO_2$ (M = Al, Ga)

Figure 1 shows X-ray diffraction patterns of (a) $CuAlO_2$ obtained in this study and (b) specimen after heating (a) at 900 °C for 12 h in air. All the peaks depicted in Fig. 1a could be indexed as hexagonal symmetry with $a = 2.857$ Å and $c = 16.94$ Å, indicating 3R delafossite type structure [13]. The different diffraction pattern was observed after the heat-treatment as shown in Fig. 1b, suggesting that $CuAlO_2$ was not thermodynamically stable at 900 °C in air. The diffraction peaks of Fig. 1b could be identified as mixture of CuO and $CuAl_2O_4$ [14], indicating that following chemical reaction involving oxidation occurred by the heat-treatment.

$$4CuAlO_2 + O_2 \rightarrow 2CuO + 2CuAl_2O_4 \quad (1)$$

Figure 2a shows X-ray diffraction pattern of $CuGaO_2$ prepared in this study. All the diffraction peaks could be indexed as 3R delafossite hexagonal structure with $a = 2.976$ Å and $c = 17.16$ Å. Since diffraction pattern of the specimen after the heat-treatment at 700 °C for 12 h could be assigned as a mixture of CuO and $CuGa_2O_4$ [15] as depicted in Fig. 2b, following chemical reaction could be proposed at the heat-treatment.

$$4CuGaO_2 + O_2 \rightarrow 2CuO + 2CuGa_2O_4 \quad (2)$$

Since thermodynamic functions of all the chemical species in 1 and 2 are listed in thermodynamic calculation program, MALT-2 [12], Ellingham diagram of reaction (1) and (2) can be calculated and displayed as solid and dashed lines in Fig. 3, respectively. In Fig. 3, temperatures and log $P(O_2)$ where three phases, $CuAlO_2$–$CuAl_2O_4$–CuO and $CuGaO_2$–$CuGa_2O_4$–$Cu_2O$, coexist proposed by Jacob and Alcock [9] and Gall and Cann [10] are represented by circles and triangles, respectively. Our calculated Ellingham diagram of reaction (2) showed fair agreement with the reported calculation [10]. However, difference was

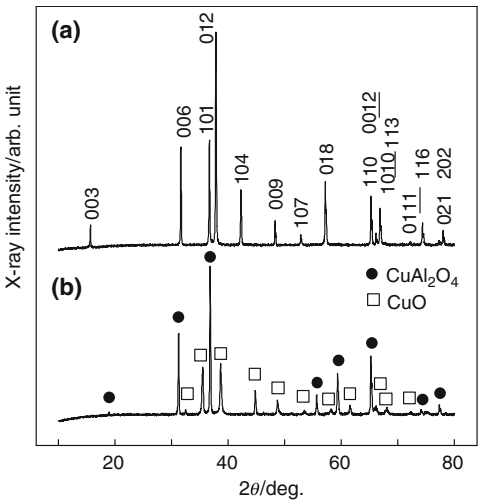


**Fig. 1** X-ray diffraction patterns of $CuAlO_2$ **a** prior to heat-treatment and **b** after heating at 900 °C for 12 h in air. Diffraction pattern of (**a**) can be indexed as hexagonal delafossite structure with $a = 2.857$ Å and $c = 16.94$ Å. Diffraction peaks of (**b**) can be indexed as either CuO (*open square*) or $CuAl_2O_4$ (*closed circle*)

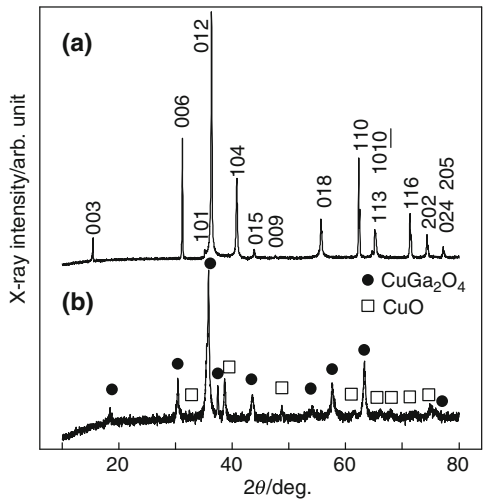


**Fig. 2** X-ray diffraction patterns of $CuGaO_2$ **a** prior to heat-treatment and **b** after heating at 700 °C for 12 h in air. Diffraction pattern of (**a**) can be indexed as hexagonal delafossite structure with $a = 2.976$ Å and $c = 17.16$ Å. Diffraction peaks of (**b**) can be indexed as either CuO (*open square*) or $CuGa_2O_4$ (*closed circle*)

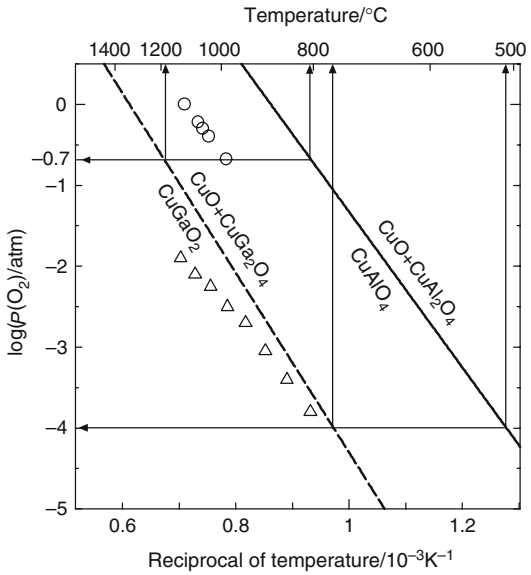


**Fig. 3** Ellingham diagram of reaction (1) $4CuAlO_2 + O_2 \rightarrow 2CuO + 2CuAl_2O_4$ (*solid line*) and (2) $4CuGaO_2 + O_2 \rightarrow 2CuO + 2CuGa_2O_4$ (*dashed line*) calculated by using program MALT-2 [12]. Temperatures and log$P(O_2)$ where three phases of $CuAlO_2$–$CuAl_2O_4$–CuO proposed by Jacob and Alcock [9] and $CuGaO_2$–$CuGa_2O_4$–$Cu_2O$ by Gall and Cann [10] are represented by *circles* and *triangles*, respectively

observed between phase boundaries of reaction (1) obtained with our calculation and measurement of electromotive force [9]. According to our calculation, thermodynamically stable region of $CuAlO_2$ in air (log $P(O_2)$ of about −0.7) is above 800 °C, whereas $CuAlO_2$ is not thermodynamically stable and decomposed to CuO and $CuAlO_2$ below 800 °C in air. Since reaction (1) occurs by heat-treatment at 900 °C in air as shown in Fig. 1, it is concluded that there is some deviation of temperature in our calculation and that experimentally obtained boundary as depicted by circles in Fig. 3 is more accurate. The deviation is probably due to deficient accuracy of thermodynamic function of $CuAlO_2$ and $CuAl_2O_4$ listed in MALT2; however, we regard that calculated Ellingham diagram can be used for semi-quantitative estimation of thermodynamic stability. Comparing two phase boundary of reaction (1), namely $CuAlO_2$, and (2) namely $CuGaO_2$, depicted in Fig. 3, it can be concluded that thermodynamic stability of $CuAlO_2$ is higher than that of $CuGaO_2$ since stable region of $CuAlO_2$ is wider than that for $CuGaO_2$. It is also prospected from our calculation in Fig. 3 that $CuGaO_2$ cannot be prepared in air since temperature above 1,200 °C is necessary, which must be probably above the melting point. In fact, $CuGaO_2$ could not be prepared by heat-treatment at 1,100–1,200 °C in air. Also, it is prospected that $CuGaO_2$ can be prepared by reducing log $P(O_2)$ as low as −4 by $N_2$ flow since it become thermodynamically stable above 800 °C, showing correspondence with our preparation conditions.

Although $CuAlO_2$ is not thermodynamically stable below 800 °C in air according to Fig. 3, it can be prepared by heating the mixture of CuO and α-$Al_2O_3$ at 1,200 °C in air followed by cooling at 200 °C/h in the same atmosphere. Also, in spite of thermodynamical instability of $CuGaO_2$ below 800 °C in $N_2$ atmosphere, it can be prepared by heating the mixed powder at 1,100 °C in $N_2$ followed by cooling at 200 °C/h in the same atmosphere. These indicate that reaction kinetics of (1) and (2) below 800 °C in air or $N_2$ are slow; however, they have not been measured so far. In the next section, kinetic stability of $CuAlO_2$ and $CuGaO_2$ has been evaluated quantitatively.

## Kinetic stability of $CuMO_2$ (M = Al, Ga)

Since oxidation kinetics of powder can also be affected by particle size, the particle size distributions are required to be similar in order to compare chemical reactivity for oxidation as a material. Figure 4 shows distribution of particle size of $CuAlO_2$ and $CuGaO_2$ powder employed for the measurement of reaction rate of (1) and (2). Similar particle distribution with peak of 0.4 and 3 μm was observed, indicating that the difference of reaction rate evaluated in this study was not attributed to difference of particle size but to difference of reactivity between $CuAlO_2$ and $CuGaO_2$.

Figure 5a shows mass variation of $CuAlO_2$ by time at constant temperatures in air. At 357 °C, no mass variation was observed, indicating no oxidation due to slow kinetics.

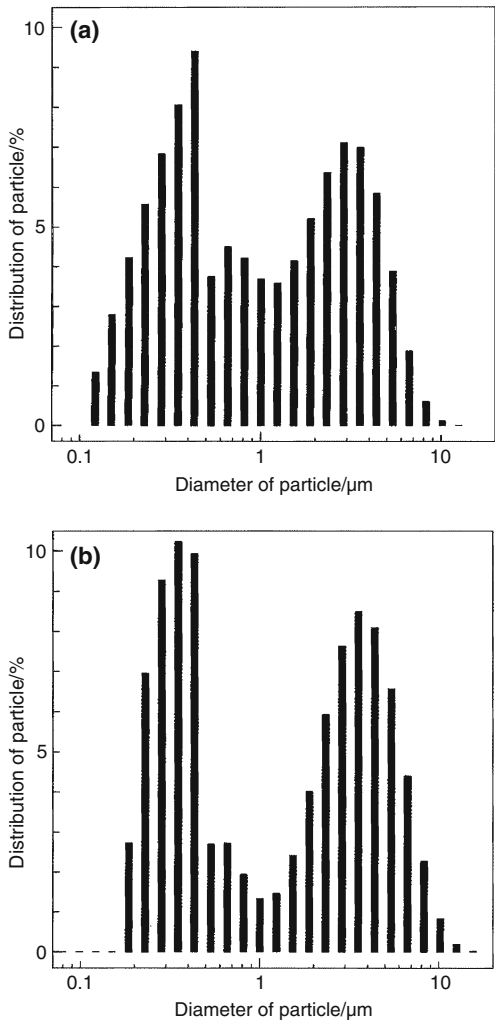


**Fig. 4** Distribution of particle size of **a** $CuAlO_2$ and **b** $CuGaO_2$ powder employed for measurement of mass variation by time at various temperatures. Similar distribution was observed

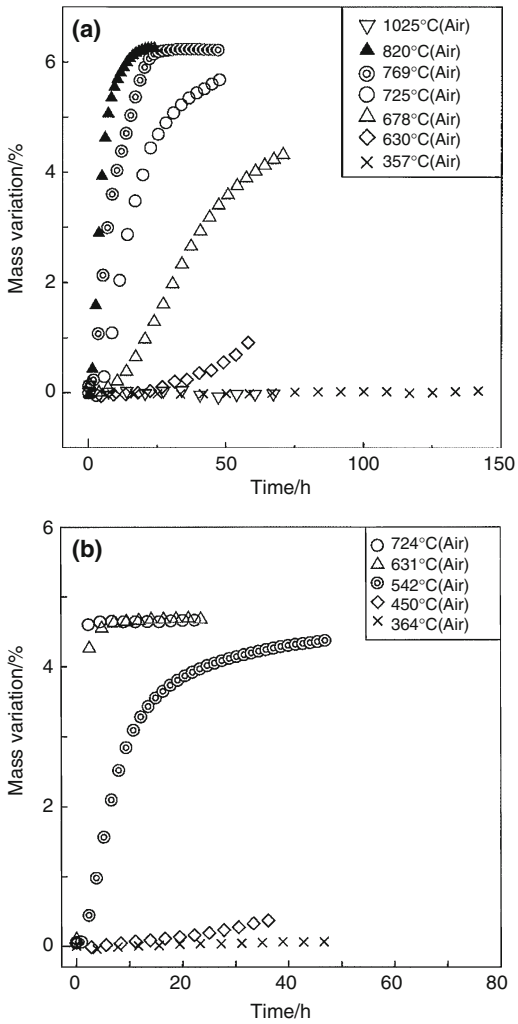


**Fig. 5** Time dependence of mass of **a** $CuAlO_2$ and **b** $CuGaO_2$ powder at various temperatures in air

Increase of mass due to reaction (1) was observed above 630 °C and reaction rate increased with increase of temperature in the range of 630–820 °C. Mass increase of 6.5% should be observed when reaction (1) is completed, which was observed as saturation of 6.2% at 769 and 820 °C. The origin of the difference from ideal value is not identified; however, it can be ascribed to experimental error due to small quantity of specimens as low as 30 mg. However, more than 15 h is necessary to complete the reaction for about 30 mg of the specimen even at 820 °C, showing slow kinetics of reaction (1). At 1,025 °C, no mass variation was observed showing agreement with thermodynamically stable region of $CuAlO_2$ depicted in Fig. 3.

Figure 5b shows mass variation of $CuGaO_2$ by time at constant temperatures in air. At 364 °C, no mass variation was observed, indicating no decomposition due to slow kinetics as well as $CuAlO_2$. Increase of mass by time due to reaction (2) was observed above 450 °C and reaction rate increased with increase of temperature in the range of 450–724 °C. Mass increase of 4.8% should be observed when reaction (2) is completed, which was observed as saturation of 4.6% at 724 °C and 631 °C. Especially, reaction (2) at 724 °C completed in about 0.5 h. Thus, it was revealed that kinetic stability of $CuAlO_2$ was higher than that of $CuGaO_2$.

For quantitative estimation of kinetic stability, mass variation, $\Delta w$, depicted as vertical axes of Fig. 5 was converted to reaction ratio, $\alpha$ using $\alpha = \Delta w/\Delta w_{sat}$, where $\Delta w_{sat}$ denotes saturated mass variation. Assuming reaction rate, $v$, is proportional to amount of substance of $CuMO_2$ (M = Al, Ga) under constant $P(O_2)$, i.e.,

$$v = -\frac{d[\mathrm{CuMO_2}]}{dt} = k'P(\mathrm{O_2})[\mathrm{CuMO_2}] = k[\mathrm{CuMO_2}] \quad (\mathrm{M} = \mathrm{Al,Ga}), \tag{3}$$

amount of substance of $CuMO_2$, CuO, and $CuM_2O_4$ can be expressed as $A\exp(-kt)$, $\frac{A}{2}\{1-\exp(-kt)\}$, and $\frac{A}{2}\{1-\exp(-kt)\}$, respectively ($A$: initial amount of substance of $CuMO_2$, $k$: rate constant). It is found from tedious calculation that $\alpha$ is equal to $1-\exp(-kt)$. Therefore, linear relationship with proportional constant of $-k$ should be observed between $\ln(1-\alpha)$ and time, $t$, if kinetic formula represented as (3) is applicable. Figure 6 shows time dependence of $\ln(1-\alpha)$ for (a) $CuAlO_2$ and (b) $CuGaO_2$ at various temperatures calculated from the data shown in Fig. 5. Almost linear relationships were observed, indicating that reaction model depicted as Eq. 3 could be applicable for reactions of (1) and (2). From the slopes depicted in Fig. 6, rate constant, $k$, can be estimated.

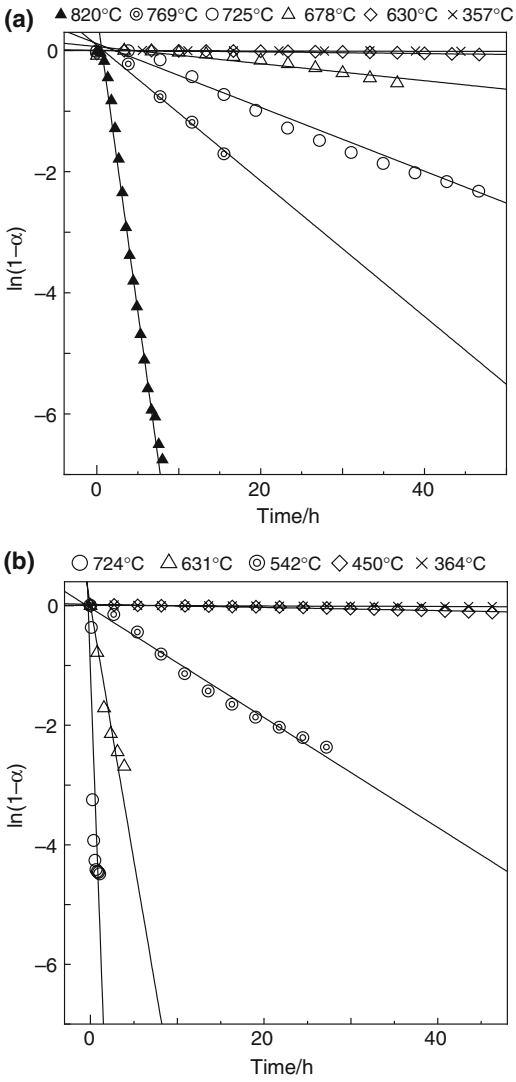


**Fig. 6** Dependence of $\ln(1-\alpha)$ on time for **a** $CuAlO_2$ and **b** $CuGaO_2$ at various temperatures in air. $\alpha$ denotes reaction ratio calculated from vertical axis of Fig. 5. Almost linear relationships were observed regardless of temperature and specimens

Figure 7 shows calculated log $k$ as a function of reciprocal of temperature. Almost linear relationships were obtained, indicating that activation energy of reaction (1) and (2) was almost independent on temperature. In the temperature range between room temperature and 800 °C, where mixture of CuO and $CuM_2O_4$ is thermodynamically stable, smaller $k$ was observed for reaction (1), namely $CuAlO_2$, than (2), namely $CuGaO_2$, indicating that kinetic stability of $CuAlO_2$ was higher than that of $CuGaO_2$. Higher kinetic stability of $CuAlO_2$ can also be supported from activation energy calculated from the slope of Fig. 7. The activation energy for reaction (1), namely $CuAlO_2$, was 266 kJ/mol, which was higher than that for reaction (2), namely $CuGaO_2$, of 128 kJ/mol. It can be concluded that single phases of $CuAlO_2$ and $CuGaO_2$ can be prepared with heat-treatment at 1,200 °C in air and 1,100 °C in $N_2$, respectively, followed by cooling with rate of 200 °C/h because the rates of the reaction (1) and (2) below 800 °C under each preparation atmosphere are slow enough.

## Explanation of TG-DTA curves of $CuMO_2$ (M = Al, Ga)

As a simple estimation method for analyzing stability of materials, TG-DTA measurements have been frequently employed. In this section, TG-DTA curves of $CuAlO_2$ and $CuGaO_2$ measured in air at heating rate of 10 °C/min,

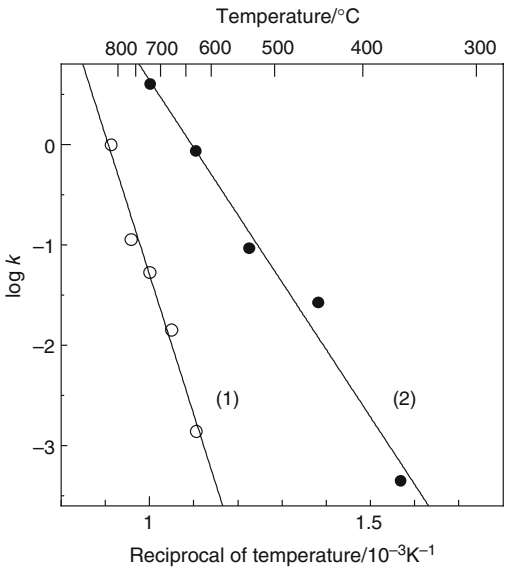


**Fig. 7** Arrhenius plot of rate constant, $k$, of the reaction (1) $4CuAlO_2 + O_2 \rightarrow 2CuO + 2CuAl_2O_4$ (*open circle*) and (2) $4CuGaO_2 + O_2 \rightarrow 2CuO + 2CuGa_2O_4$ (*closed circle*) in air. Almost linear relationships indicating constant activation energy were obtained

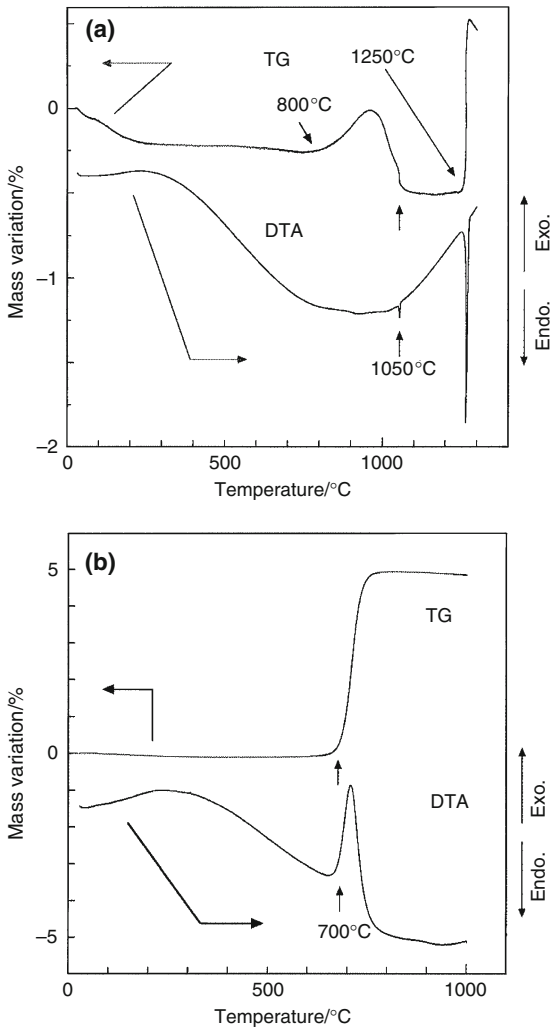


**Fig. 8** TG-DTA curves of **a** $CuAlO_2$ and **b** $CuGaO_2$ at heating procedure with rate of 10 °C/min in air

shown in Fig. 8, are explained using thermodynamic and kinetic stability described above.

In TG curve of $CuAlO_2$ depicted in Fig. 8a, gradual mass decrease was observed from room temperature to 200 °C. It can be ascribed to desorption of adsorbed specimen such as $H_2O$ and $CO_2$. Considering that mixture of CuO and $CuAl_2O_4$ is thermodynamically stable at low temperatures in air, mass increase from 800 °C can be attributed to beginning of reaction (1). From about 950 °C, mass decreased again, suggesting that inverse reaction of (1) started due to thermodynamical stability of $CuAlO_2$ at the higher temperatures than 950 °C. However, no signal was observed in DTA curve around 800 °C nor around 950 °C, which could be ascribed to slow kinetics of reaction (1). At 1,050 °C, discontinuous mass decrease and endothermic signal were observed. From the reported Ellingham diagram of $4CuO \rightarrow 2Cu_2O + O_2$ [8] and comparison of reported TG-DTA data of CuO [16], it can be ascribed to reduction of trace amount of CuO, which generated as reaction (1), to $Cu_2O$. The origin of smaller sample mass at the range of 1,100–1,200 °C than that of 300–800 °C of about 0.25% could not be identified; one possible cause might be experimental error due to small quantity of specimen. Endothermic peak at 1,250 °C can be assigned as the melting point of $CuAlO_2$.

TG-DTA curve of $CuGaO_2$ in air depicted in Fig. 8b showed different behavior from that for $CuAlO_2$. Mass increase from 700 °C was observed indicating that reaction (2) started due to thermodynamic instability of $CuGaO_2$ at the temperature in air. At 700 °C, exothermic peak due to reaction (2) was also detected, showing correspondence with higher kinetics of reaction (2) than that of reaction (1). At the temperatures higher than 800 °C, the mass was saturated to about 4.9%, which was identified that reaction (2) was completed and that mixture of $CuGa_2O_4$ and CuO was thermodynamically more stable than $CuGaO_2$ in air below 1,000 °C as shown in Fig. 3.

## Conclusions

It has been revealed that $CuAlO_2$ and $CuGaO_2$ are thermodynamically unstable in air below 900 °C and 1,200 °C, respectively, and that thermodynamical stability of $CuAlO_2$ is higher than that of $CuGaO_2$. They are oxidized according to the chemical reaction, $4CuMO_2 + O_2 \rightarrow 2CuO + 2CuM_2O_4$ (M = Al, Ga), under thermodynamically unstable temperatures and atmospheres if the reaction kinetics are high enough. Owing to slow kinetics of the oxidation reaction of $CuAlO_2$ in air and $CuGaO_2$ in $N_2$ with $\log P(O_2)$ of about −4, single phases of $CuAlO_2$ and $CuGaO_2$ can be prepared by heating the mixture of raw materials under thermodynamically stable conditions, such as at 1,200 °C in air and at 1,100 °C in $N_2$, respectively, followed by cooling rate of 200 °C/h.

Reaction model that kinetics of the oxidation reaction in air was proportional to amount of substance of $CuMO_2$ could be applicable. Obtained rate constants indicate higher kinetic stability of $CuAlO_2$ than that of $CuGaO_2$. Activation energies of $CuAlO_2$ and $CuGaO_2$ oxidation reactions estimated from Arrhenius plots were 266 and 128 kJ/mol, respectively, showing also higher kinetic stability of $CuAlO_2$ than $CuGaO_2$. The difference of TG-DTA curve in air between $CuAlO_2$ and $CuGaO_2$, such as appearance of exothermic peak due to oxidation reaction, could be explained from difference of kinetics of the oxidation reaction.

**Acknowledgements** The authors acknowledge Prof. K. Endoh (College of Humanities and Sciences, Nihon University) for the

measurement of particle size distribution with laser diffraction particle size analyzer.

## References


1. Kawazoe H, Yasukawa M, Hyodo H, Kurita M, Yanagi H, Hosono H. P-type electrical conduction in transparent thin films of $CuAlO_2$. Nature. 1997;389:939–42.
2. Yanagi H, Kawazoe H, Kudo A, Yasukawa M, Hosono H. Chemical design and thin film preparation of p-type conductive transparent oxides. J Electroceramics. 2000;4:407–14.
3. Kato S, Fujimaki R, Ogasawara M, Wakabayashi T, Nakahara Y, Nakata S. Oxygen storage capacity of $CuMO_2$ (M = Al, Fe, Mn, Ga) with a delafossite-type structure. Appl Catal B Environ. 2008;89:183–8.
4. Jacob A, Parent C, Boutinaud P, Le Flem G, Doumerc JP, Ammar A, et al. Luminescent properties of delafossite-type oxides $LaCuO_2$ and $YCuO_2$. Solid State Commun. 1997;103:529–32.
5. Tsuboi N, Hoshino T, Ohara H, Suzuki T, Kobayashi S, Kato K, et al. Control of luminescence and conductivity of delafossite-type $CuYO_2$ by substitution of rare earth canon (Eu, Tb) and/or Ca canon for Y cation. J Phys Chem Solids. 2005;66:2134–8.
6. Takahashi H, Motegi Y, Tsuchigane R, Hasegawa M. Pressure effect on the antiferromagnetic transition temperature in $CuFeO_2$. J Mag Mag Mater. 2004;272:216–7.
7. Yanagi H, Ueda K, Ohta H, Orita M, Hirano M, Kawazoe H, et al. Fabrication of all oxide transparent p-n homojunction using bipolar $CuInO_2$ semiconducting oxide with delafossite structure. Solid State Commun. 2002;121:15–7.
8. Hashimoto T, Koinuma H, Kishio K. Thermodynamic estimation of oxidation ability of various gases used for the preparation of superconducting films at high-vacuum. Jpn J Appl Phys. 1991;30:1685–6.
9. Jacob KT, Alcock CB. Thermodynamics of $CuAlO_2$ and $CuAl_2O_4$ and phase-equilibria in system $Cu_2O$–CuO–$Al_2O_3$. J Am Ceram Soc. 1975;58:192–5.
10. Gall RB, Cann DP. High temperature phase equilibria in the $Cu_2O$–$Ga_2O_3$–$In_2O_3$ system. Ceram Eng Sci Proc. 2003;24:143–8.
11. Jacob KT, Alcock CB. Thermodynamics and phase-equilibria in system $Cu_2O$–CuO–$Ga_2O_3$. Revue Inter Hautes Temp Refractaires. 1976;13:37–42.
12. Yokokawa H, Yamauchi S, Matsumoto T. Thermodynamic database MALT for windows with gem and CHD. Calphad. 2002;26:155–66.
13. Ishiguro T, Kitazawa A, Mizutani N, Kato M. Single-crystal growth and crystal-structure refinement of $CuAlO_2$. J Solid State Chem. 1981;40:170–4.
14. Areán CO, Viñuela JSD. Structural study of copper-nickel aluminate ($Cu_xNi_{1-x}Al_2O_4$) spinels. J Solid State Chem. 1985;60:1–5.
15. Stone FS, Areán CO, Viñuela JSD, Platero EE. Structural characterization of cadmium copper gallium oxide ($Cd_xCu_{1-x}Ga_2O_4$) Spinels. J Chem Soc Faraday Trans. 1985;81:1255–61.
16. Tsuchida T, Furuichi R, Sukegawa T, Furudate M, Ishii T. Thermoanalytical study on the reaction of the CuO-$Al_2O_3$($\eta$, $\gamma$ and $\alpha$) systems. Thermochim Acta. 1984;78:71–80.